CHEMICAL ENGINEERING TRANSACTIONS
VOL. 81, 2020
A publication of AIDIC
The Italian Association of Chemical Engineering
Online at www.cetjournal.it
Guest Editors: Petar S. Varbanov, Qiuwang Wang, Min Zeng, Panos Seferlis, Ting Ma, Jiří J. Klemeš
Copyright © 2020, AIDIC Servizi S.r.l.
ISBN 978-88-95608-79-2; **ISSN** 2283-9216
DOI: 10.3303/CET2081001

Numerical Analysis of Semi-dry Flue Gas Desulfurization Process in the 3D Spouted Bed

Jiali Du[a], Kai Yue[a], Feng Wu[a,*], Xiaoxun Ma[a], Zhiquan Hui[b], Maodong Li[b]

School of Chemical Engineering, Northwest University, Xi' an, China
Guangzhou Special Pressure Equipment Inspection and Research Institute, Guangzhou 510663, China
wufeng@nwu.edu.cn

This paper presents a numerical study of gas-solid two-phase flow and water vaporization in a 3D powder-particle spouted bed (PPSB) by means of the combined approach of the Eulerian-Eulerian two-fluid model (TFM) and kinetic theory of granular flows (KTGF). The simulation shows that the gas temperature in the injection area is higher than water and particles, and the three-phase temperatures in other areas are similar. The water vaporization rate is higher at the junction of the injection area and the annulus area, lower in the center of the injection area, and lowest in the annulus area. By increasing gas velocity and liquid temperature, reducing gas humidity, promoting water vaporization.

1. Introduction

In recent years, a large amount of coal-fired emissions cause serious air pollution and the degree of pollution continues to increase. It is necessary to control the SO_2 content to reduce the environmental pollution (Chang, 2020). The semi-dry flue gas desulfurization (FGD) process with a powder-particle spouted bed (PPSB) has become a new type of desulfurization technology with great application prospects. Liu et al. (2008) focused on the effect of hydrogen peroxide solution concentration and various factors on the desulfurization efficiency in the semi-dry FGD progress. However, the experimental research cannot observe the parameters like material velocity, temperature and reaction rate in the bed. The simulation method can obtain these data and better understand the mechanism of the desulfurization process, which has been widely recognized as a useful tool by researchers (Hosseini et al., 2015). Hosseini et al. (2009) simulated a spouted bed containing non-porous draft tube by using a multi-fluid Eulerian-Eulerian approach incorporating the kinetic theory of granular flows (KTGF). Simulation indicates that the model can be employed for both mono-size and multi-size particles reasonably. Wu et al. (2020) simulated the process of water vaporization and semi-dry FGD in 2D PPSB, based on gas-solid two-phase flow, computational fluid dynamics (CFD) combined with the two-fluid model (TFM) was used for simulation of water vaporization. No mathematical modelling has been reported for the semi-dry FGD process in a 3D PPSB at present. The semi-dry FGD process with a PPSB is a complex multi-phase reaction system, water provides a place for the reaction and affects the desulfurization reaction. It is of great significance to study the water vaporization process (Ma et al., 1999), which is the basis for further studying the reaction characteristics in the system and the process of powder entrapment (Ma et al., 2000).
Based on the above discussions, this paper presents a numerical study of gas-solid two-phase flow and water vaporization by means of the combined approach of the Eulerian-Eulerian TFM and KTGF in a 3D PPSB.

2. Numerical method

2.1 Hydrodynamic model

The governing equations and the associated constitutive models of the TFM in the simulation of PPSB are summarized in this section.
The mass conservation equation is expressed as:

Paper Received: 27 April 2020; Revised: 28 May 2020; Accepted: 01 June 2020
Please cite this article as: Du J., Yue K., Wu F., Ma X., Hui Z., Li M., 2020, Numerical Analysis of Semi-dry Flue Gas Desulfurization Process in the 3D Spouted Bed, Chemical Engineering Transactions, 81, 1-6 DOI:10.3303/CET2081001

$$\frac{\partial}{\partial \mathrm{t}}\left(\alpha_{\mathrm{i}} \rho_{\mathrm{i}}\right)+\nabla \cdot\left(\alpha_{\mathrm{i}} \rho_{\mathrm{i}} v_{\mathrm{i}}\right)=0 \tag{1}$$

Where i represents the gas or particle phase.

The gas momentum conservation equation is given as:

$$\frac{\partial}{\partial \mathrm{t}}\left(\alpha_g \rho_g v_g\right)+\nabla \cdot\left(\alpha_g \rho_g v_g v_g\right)=-\partial_g \nabla p_g+\partial_g \rho_g g+K_{gs}\left(v_s-v_g\right)+\nabla \cdot \tau_g \tag{2}$$

Where K_{gs} is the drag coefficient of the gas-particle phase, and τ_{g} is the gas stress tensor.

The particle momentum conservation equation is given as:

$$\frac{\partial}{\partial \mathrm{t}}\left(\alpha_s \rho_s v_s\right)+\nabla \cdot\left(\alpha_s \rho_s v_s v_s\right)=-\partial_s \nabla p_s+\partial_s \rho_s g+K_{gs}\left(v_g-v_s\right)+\nabla \cdot \tau_s \tag{3}$$

The energy conservation equation is calculated by:

$$\frac{\partial}{\partial \mathrm{t}}\left(\alpha_i \rho_i h_i\right)+\nabla \cdot\left(\alpha_i \rho_i v_i h_i\right)=-\alpha_i \frac{\partial P_i}{\partial t}+\tau \cdot \nabla v_i-\nabla \cdot q_i \tag{4}$$

The transport equation for granular temperature, θ (fluctuation kinetic energy of particles) is given as:

$$\frac{3}{2}\left[\frac{\partial}{\partial t}\left(\varepsilon_S \rho_S \theta\right)+\nabla \cdot\left(\varepsilon_S \rho_S \theta\right) v_S\right] I=\left(-\nabla p_S \bar{I}+\tau_S\right): \nabla v_S+\nabla \cdot\left(k_S \nabla \theta\right)-\gamma_S+\phi_S+D_{gs} \tag{5}$$

The drag model as given by Gidaspow (Gidaspow and Tsuo, 1990) is expressed as:

$$\beta_{gs}=\begin{cases}\frac{3}{4} C_D \frac{\alpha_s \alpha_g \rho_g\left|u_g-u_s\right|}{d_s} \alpha_g^{-2.65}, \alpha_g \geq 0.8 \\ 150 \frac{\alpha_s^2 \mu_g}{\alpha_g d_s^2}+1.75 \frac{\alpha_s \rho_g\left|u_g-u_s\right|}{d_s}, \alpha_g<0.8\end{cases} \tag{6}$$

Where

$$C_D=\begin{cases}\frac{24}{\alpha_g \mathrm{Re}}\left[1+0.15\left(\alpha_g \mathrm{Re}\right)^{0.687}\right] & \mathrm{Re} \leq 1000 \\ 0.44 & \mathrm{Re}>1000\end{cases} \tag{7}$$

2.2 Water evaporation model

The water evaporation rate per unit area of desulfurization slurry (Haywood et al., 1989) is expressed as:

$$m_a=\frac{D_g}{2 R_d} Sh \cdot \rho_{total} \cdot B_M \tag{8}$$

Sh is the Sherwood dimensionless number, which is expressed as:

$$Sh=\left(2.0+0.552 Re^{\frac{1}{2}} Sc^{\frac{1}{3}}\right)\left(1+B_M\right)^{-\frac{2}{3}} \tag{9}$$

where B_M is the difference between mass fraction in the gas-liquid interface saturation vapor and mass fraction of water vapor in the gas phase subject value, which can be expressed as:

$$B_M=\frac{Y_{sat}\left(1-\varphi\right)}{1-Y_{sat}} \tag{10}$$

2.3 Simulation set-up

Figure 1 is a simplified diagram of the size of the spouted bed. Bottom of gas inlet and top of water inlet are

defined as speed inlets, the boundary condition of the top ring is defined as pressure outlet, and the other faces are defined as wall. The superficial air velocity is 0.7 m/s, the direction is vertical boundary surface, inlet gas T = 520 K. The slurry velocity is 0.026 m/s, and slurry T = 300 K.

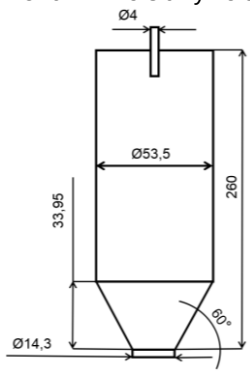

Figure 1: Simplified size of spouted bed

Table 1: Size parameters of the spouted bed and particle parameters

Parameter	Value	Parameter	Value
Cylinder diameter	53.5 mm	Nozzle diameter	14.3 mm
Cone angle	60 °	Cone height	33.95 mm
Media particle volume fraction	0.55	Maximum particle volume fraction	0.55
Min jet speed	0.56 m/s	Medium particle density	2,700 kg/m^3
Media particle recovery factor	0.9	Particle diameter	460 μm
Media particle friction angle	28.7 °	Operating pressure	101,325 Pa

Table 2: Physical properties of gas phase

Chemical formula of components	H_2O	SO_2	N_2	O_2
Density (kg/m^3)	0.554	2.77	1.138	1.3
Heat capacity at constant pressure (J/kg-K)	2,014	622.28	1,040.67	919.31
Dynamic viscosity (kg/m-s)	1.34×10^{-5}	1.2×10^{-5}	1.66×10^{-5}	1.92×10^{-5}
Coefficient of thermal conductivity (W/m-K)	0.026	0.01	0.024	0.025
Molar mass (kg/kmol)	18.015	64.065	28.013	31
Standard enthalpy of formatio (J/kmol)	-2.418×10^8	-2.969×10^8	0	0
Reference temperature (K)	298.15	298.15	298.15	298.15

Table 1 shows the size parameters of the bed and particle parameters in the simulation, and Table 2 shows the physical properties of gas. On the basis of stable gas-solid two-phase flow, along with the application of the user defined function (UDF) method to realize water heat and mass transfer by considering evaporation in the simulation process. The SIMPLE algorithm is used for the pressure-velocity coupling. A first-order upwind discretization scheme is used for the phase volume fraction, and a second-order upwind discretization scheme is used for momentum, turbulence kinetic energy and turbulence dissipation rate equations.

3. Results and discussion

3.1 Flow of gas and particle in spouted bed

In this section, the flow conditions in the bed are studied in terms of particle volume fraction, particle pseudo-temperature, radial and axial velocity of the gas during the two-phase flow.

Figure 2a shows the contours of particle volume fraction in the spouted bed. It can be seen that the gas first forms a larger bubble in the bed. As the gas enters the bed, the bubbles continue to grow and move upwards against the particles. At the same time, some particles flow downward along the wall, and the gas layer breaks through the particle layer in 0.6 s to form an approximately continuous gas phase that complete the first spurt process. Figure 2b displays the distribution of particles pseudo-temperature along the radial distance at the height of 0.04 m, 0.08 m and 0.12 m. Particle pseudo-temperature is an important parameter to evaluate the degree of particle pulsation. At 0.04 m, the pseudo-temperature of the particles in the injection area is higher, and then gradually decreases, indicates that the pulsation intensity of the particles is greater in the injection

area at this height. When the height is 0.08 m, the pseudo-temperature of the particles is close to zero with little change. At the height of 0.12 m, at the center of the fountain area, the particle temperature is zero. Near the wall, the temperature increases a little bit.

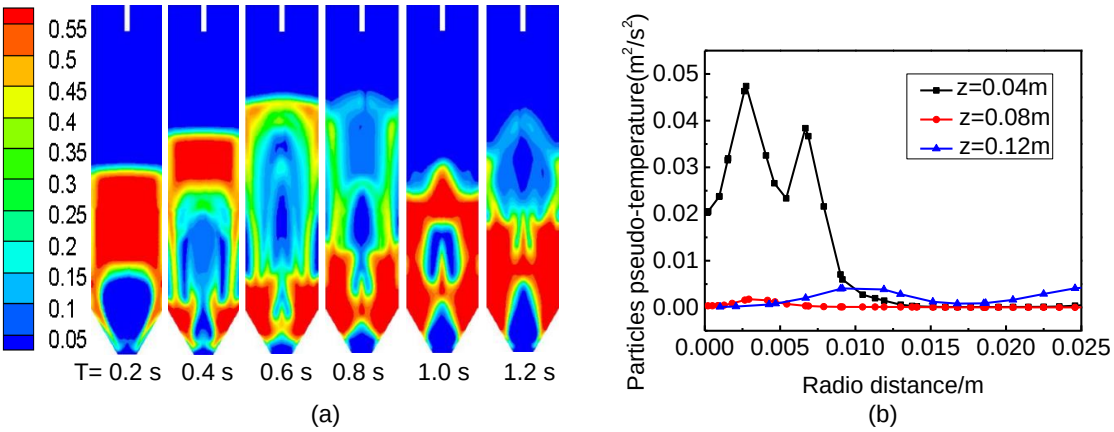

Figure 2a: Contours of particle volume fraction, 2b: Distribution of particles pseudo-temperature along the radial distance at different heights

Contours of radial distribution of gas velocity in the 3D spouted bed is shown in Figure 3a. The gas flows in a reverse direction at the junction of the cone and the cylinderthe and is symmetrical along the central axis. This is because the particles gather towards the center under the combined effect of the pressure of the upper layer particles, gravity and the structure of the bed, which drives the gas to flow in the reverse direction to the center. Figure 3b shows the contours of axial distribution of gas velocity. Due to the impact of the upward moving gas, the upper layer gas velocity is larger, the gas axial velocity is larger in the upper part of the injection area of the 3D spouted bed.

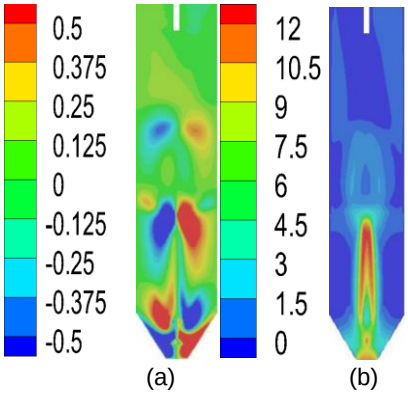

Figure 3a: Contours of radial distribution of gas velocity, 3b: Contours of axial distribution of gas velocity (m/s)

3.2 Water vaporization in spouted bed

This section mainly analyzes the temperature distributions of gas, liquid and particle, water vaporization rate distributions, and the factors that affect water vaporization rates such as gas velocity, liquid temperature and gas humidity in a 3D spouted bed.

Figure 4a is the contours of the temperature distribution of gas, liquid and particles. The gas temperature in the injection area is high for hardly containing water and particles, the heat loss is less. And there is a large amount of water in the annulus area, that the gas temperature drops a little bit, so the temperature in the annular area is low. From the contours of liquid temperature, it can be seen that the liquid temperature is higher at the junction of the fountain area and the annulus area. A certain amount of water and high-temperature gas coexist in this area, the gas transfers heat to the water. In the fountain area, the gas moves around the particles, and the three phases are fully mixed, that the temperature of the liquid drops a little. Observe the contours of particle temperature and find that the particle temperature is higher at the bottom of injection area, which reveals that a

small amount of particles are heated in this area. In other areas, the temperature of the particles is stable, because the evaporation of water absorbs a large amount of heat from the particles and gas and the particles are mixed uniformly. Figure 4b presents the contours of water vaporization rate. The figure reveals the water vaporization rate at the junction between the injection area and the annulus area is higher, because of the gas velocity and the air temperature is higher, the presence of water causes the water vaporization rate to be higher. And the water vaporization rate is lower in the center of the injection area, and lowest in the annulus area.

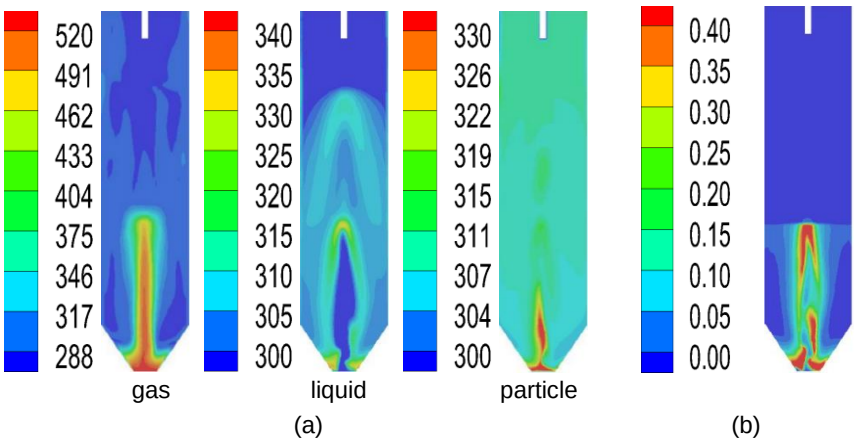

Figure 4a: Contours of the temperature distribution of gas, liquid and particles (T/K), 4b: Contours of water vaporization rate (kg·m^{-3} s^{-1})

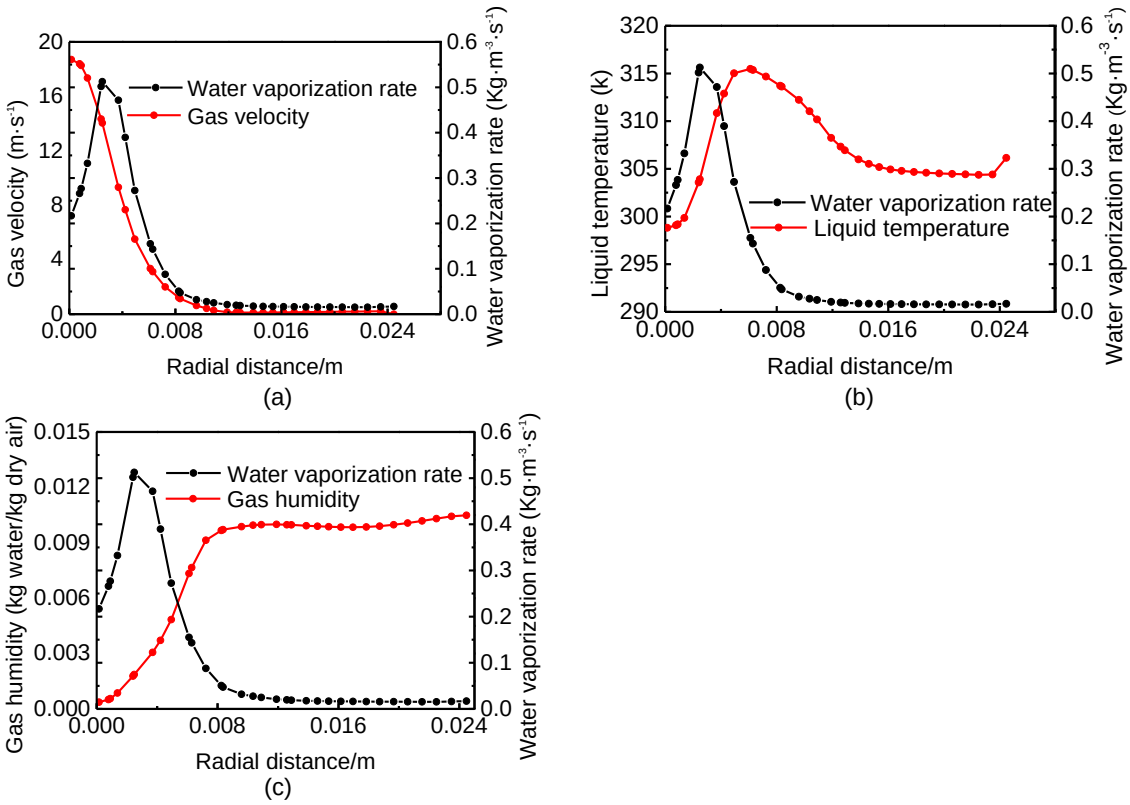

Figure 5a: Distribution of gas velocity and water vaporization rate, 5b: Distribution of liquid temperature and water vaporization rate, 5c: Distribution of gas humidity and water vaporization rate

Figure 5a shows the effect of gas velocity on the rate of water vaporization at a height of 0.03 m. The gas velocity decreases sharply along the radial distance and then maintains a relatively stable value in the annulus area, while the water vaporization rate increases sharply, then decreases sharply, and finally stays stable. The

decrease of gas velocity is due to the downward movement of the particles, which increases the driving force for mass transfer between gas and liquid, the water vaporization rate in this area is large. The reason for the decrease of the water vaporization rate is that vaporization generates water vapor, which reduces the temperature of each phase and the driving force for mass transfer. As the the effect of liquid temperature on the rate of water vaporization in Figure 5b, the temperature of liquid water and the rate of water vaporization along the radial distance have similar trends, increasing and then decreasing. But the liquid temperature is delayed compared to the water vaporization rate because the water content gradually increases along the radial distance, and the gas at the junction of the fountain area and the annulus area has the best heating effect on the water and the vaporization effect is stronger. From Figure 5c, the effect of gas humidity on the rate of water vaporization. The humidity of the gas gradually increases along the radial distance in the injection area and then maintains a stable value in the annulus area, the water vaporization rate increases sharply, then decreases sharply, and finally remains stable. This is because the lower the humidity of the gas, the greater the driving force for mass transfer, and the more it promotes vaporization.

4. Conclusions

In this paper, the gas-solid two-phase flow and the process of water vaporization in a 3D PPSB are the research objects. On the basis of establishing the model, the gas-solid flow conditions are obtained through calculation, and the UDF method is used to obtain the temperature of gas, liquid, particles and water vaporization rate distribution during the water vaporization process. These results are expected to shed light on the desulfurization reaction process, and provide data support for optimizing reactor design and improving desulfurization rate. The ultimate goal of studying 3D PPSB is to study FGD process, follow-up needs to work in this regard and explores the effect of parameters on the desulfurization rate.

Acknowledgements

This work is supported by National Natural Science Foundation of China (Grant No. 21878245), Science and technology research project of Guangzhou (Grant No. 202002030140) and Cyrus Tang Foundation.

References

Chang Z.P., 2020, Research on circulating suspension semi-dry flue gas desulfurization technology (in China), Chemical Enterprise Management, 10, 52-53.

Haywood R.J., Nafziger R., Renksizbulut M., 1989, Detailed examination of gas and liquid transient processes in convection and evaporation, Journal of Heat Transfer, 111, 495–502.

Hosseini S.H., Fattahi M., Ahmadi G., 2015, CFD Study of hydrodynamic and heat transfer in a 2D spouted bed: Assessment of radial distribution function, Journal of the Taiwan Institute of Chemical Engineers, 58, 107-116.

Hosseini S.H., Zivdar M., Rahimi R., 2009, CFD simulation of gas–solid flow in a spouted bed with a non-porous draft tube, Chemical Engineering and Processing, 48, 1539-1548.

Liu Y.B., Zhou Y.G., Peng J., Zhang M.C., 2008, Experimental study on the enhanced absorption of SO_2 with aqueous hydrogen peroxide solution based on semi-dry flue gas desulfurization (in China). Journal of Fuel Chemistry and Technology, 36(4), 474–477.

Ma X.X., Kaneko T., Guo Q.M., 1999, Removal of SO_2 from flue gas using a new semidry flue gas desulfurization process with a powder-partical spouted bed. Canadian Journal of Chemical Engineering, 77(2), 356-362.

Ma X.X., Kaneko T., Tashimo T., 2000, Use of limestone for so_2 removal from flue gas in the semidry FGD process with a powder-partical spouted bed. Chemical Engineering Science, 55(20), 4643-4652.

Tsuo Y.P., Gidaspow D., 1990, Computation of flow patterns in circulating fluidized beds. Aiche Journal, 36(6), 885-896.

Wu F., Yue K., Gao W.W., Gong M., Ma X.X., Zhou W.J., 2020, Numerical simulation of semi-dry flue gas desulfurization process in the powder-particle spouted bed, 31, 323-331.